Self-assembly of polymeric microspheres of complex internal structures

MARCIN FIALKOWSKI, AGNIESZKA BITNER AND BARTOSZ A. GRZYBOWSKI*
Department of Chemical and Biological Engineering, Northwestern University, 2145 Sheridan Road, Evanston, Illinois 60208, USA
*e-mail: grzybor@northwestern.edu

Published online: 19 December 2004; doi:10.1038/nmat1267

Self-assembly can easily produce intricate structures that would be difficult to make by conventional fabrication means. Here, self-assembly is used to prepare multicomponent polymeric microspheres of arbitrary internal symmetries. Droplets of liquid prepolymers are printed onto a water-soluble hydrogel, and are allowed to spread and coalesce into composite patches. These patches are then immersed in an isodense liquid, which both compensates the force of gravity and dissolves the gel beneath the polymers. Subsequently, the patches fold into spheres whose internal structures are dictated by the arrangement of the droplets printed onto the surface. The spheres can be solidified either thermally or by ultraviolet radiation. We present a theoretical analysis of droplet spreading, coalescence and folding. Conditions for the stability of the folded microspheres are derived from linear stability analysis. The composite microbeads that we describe are likely to find uses in optics, colloidal self-assembly and controlled-delivery applications.

Spherical microparticles are important components of many scientific technologies[1–5] and industrial products[6,7]. Most of the currently available methods for their preparation are limited to structures of spherical internal symmetry—that is, to uniform, hollow[8,9] or core-and-shell[10,11] arrangements. There has been a growing interest in developing techniques to prepare microspheres of more complex topologies. Such particles would be useful in self-assembly of intricate colloidal aggregates, in new types of optical elements[12] and displays[13,14], and in parallel chemical sensing[15]. The fabrication schemes that have so far been proposed, however, lack generality and can produce only simple spheres having roughly half of their surface modified chemically[16] or by laser radiation[17], or covered by a thin film of metal[18] or a Langmuir–Blodgett monolayer[19]. Here, we describe a versatile method based on self-assembly[20] of liquid prepolymer patches that allows the preparation of microspheres (hundreds of micrometres in diameter) of almost arbitrary internal structures, and that is easily extended to fabrication of composite particles of non-spherical (for example, concave–convex) shapes.

The method begins with printing small droplets of various hydrophobic, liquid prepolymers onto a glass slide covered with a thin layer of a water-soluble gel. Once on the surface, the isolated droplets spread and ultimately coalesce into larger, composite patches. The glass slide is then immersed in an aqueous salt solution isodense with the prepolymers, which (i) underetches the surface below the patches and (ii) effectively turns off gravity acting on the prepolymers. Underetched patches experiencing no gravity fold into microspheres that are subsequently solidified (thermally or by ultraviolet radiation). The internal structures of the microspheres depend on the positions and the sizes of the prepolymer droplets applied to the surface.

Figure 1 illustrates the technique for the case of two-component microspheres. First, a solution of hot gelatin (5 wt%) is applied to a glass surface, spin-coated at 300 r.p.m. for 30 s, and allowed to gelate under ambient conditions for 30 min. Small droplets (of radii $r_0 \approx 50$–$500\ \mu m$) of two types of liquid prepolymers are applied to the gelatin surface from a microsyringe attached to a three-dimensional translational stage. The polymers are chosen such that they are both relatively hydrophobic (typically, their surface tensions in water[21] are $\sigma_{1,2W} \approx 0.05\ N\ m^{-1}$, and those in air[21,22] are

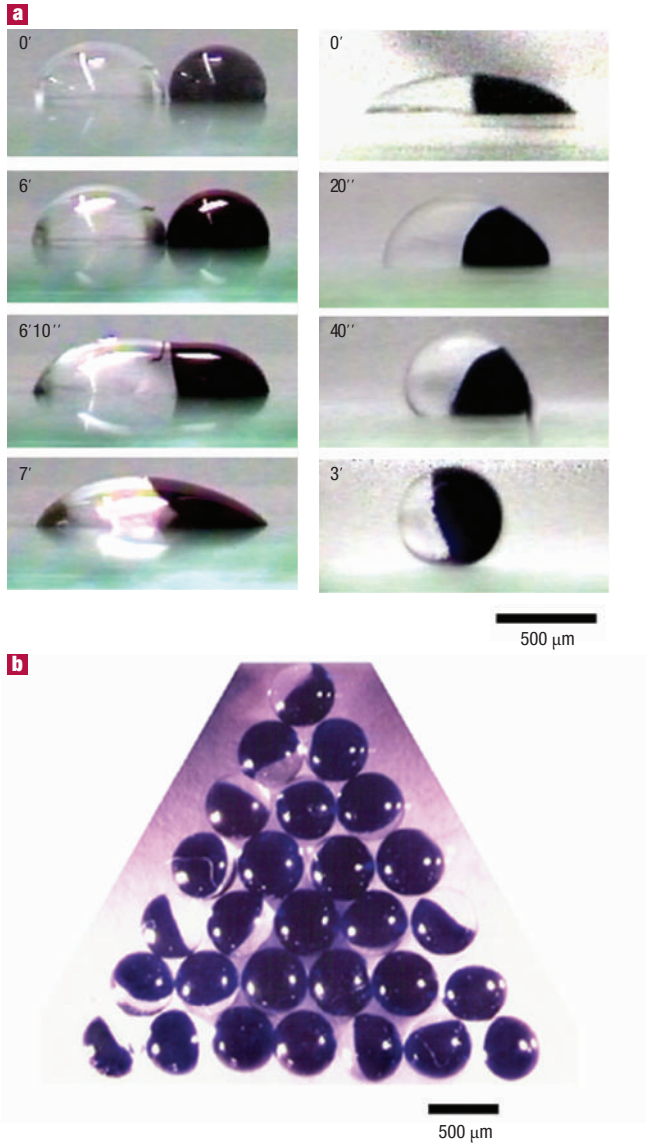

Figure 1 Spreading and folding of two-component spheres. **a**, Spreading (left column) and subsequent folding (right column) of a two-component NOA68 (clear, $\eta = 2.5$ Pa s) and NOA63 (dyed blue with Crystal Violet; $\eta = 5$ Pa s) sphere. The numbers indicate time since deposition (left column) and since initiation of the folding process (right column). **b**, Ultraviolet-cured (50 W, 5 min), two-component spheres arranged into a triangle to illustrate their monodispersity. In general, the dimensions of the spheres are controlled by the volumes of prepolymers delivered onto a surface.

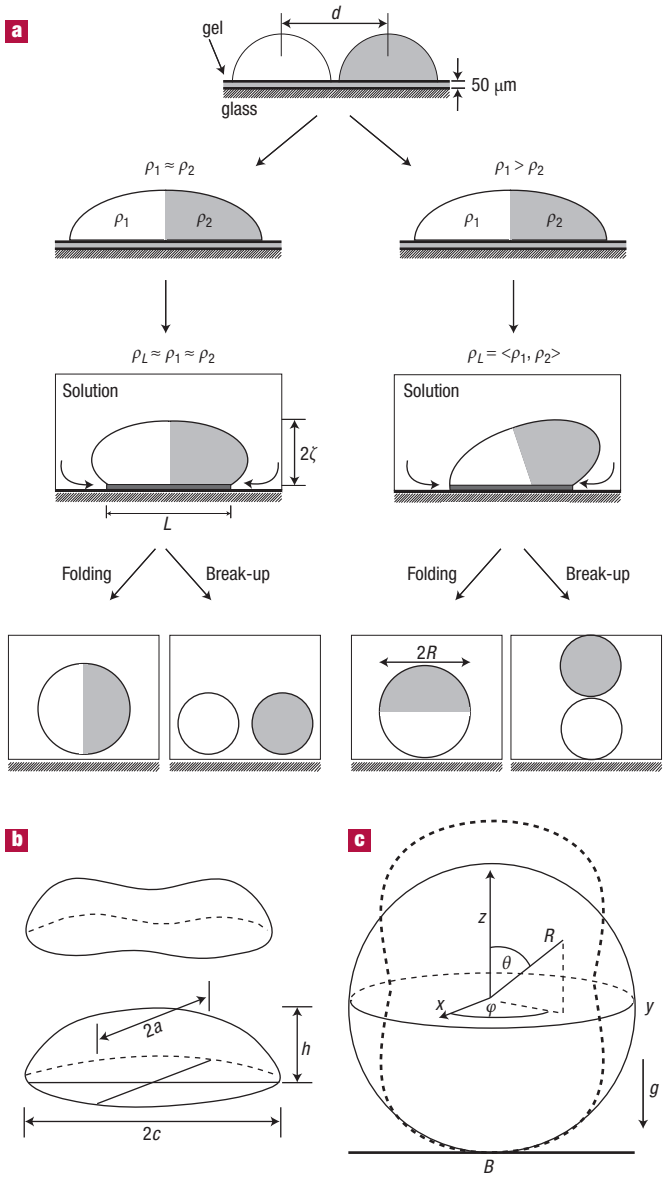

Figure 2 Schematic illustration of droplet spreading, folding and break-up. **a**, Coalescence and folding of two-component drops. Isolated droplets spread on the substrate until they merge into a composite patch. When this patch is immersed in a liquid (of density, ρ_L, close to the densities $\rho_{1,2}$ of the prepolymers), it folds into a sphere. If the two prepolymers are similar ($\rho_1 \approx \rho_2$) (left column) the patch folds into a cylindrical shape characterized by radius ζ and length $\sim L$. If $L/\zeta < 2\pi$, the patch is stable against surface fluctuations and folds properly; otherwise it breaks into two smaller droplets. If the densities of the polymer liquids differ (right column), the folding process is asymmetric and the patch evolves into a composite droplet with the lighter prepolymer occupying its top portion. If its radius, R, is small, surface tension dominates buoyancy, and the folding process is stable against fluctuations of the prepolymer–liquid interface. For larger R, the drop becomes unstable and breaks up into two parts. **b**, Ellipsoidal versus dumbbell shape of a spreading patch: Depending on the volumes of the droplets and their initial separation, the patch evolves either into a dumbbell (upper picture) or an ellipsoidal cap (lower picture) of long axis $2c$, short axis $2a$ and height h. **c**, Axisymmetric deformation (dashed line) of the surface of a spherical droplet (solid line) composed of equal amounts of two prepolymer liquids of different densities. The sphere is attached to the surface at point B, and is immersed in a liquid whose density is an arithmetic average of the densities of the two prepolymers.

$\sigma_{1,2G} \approx 0.02$–$0.03$ N m^{-1}), have low interfacial energy with respect to one another ($\sigma_{12} \approx 10^{-3}$ N m^{-1}; refs 23, 24), and can be solidified either thermally or by ultraviolet radiation. The combinations of polymers that meet these criteria and were used in our experiments were selected from a range of ultraviolet-curable polyurethanes (Norland Optical Adhesives, density $\rho = 1.19$ g cm^{-3}), thermally curable siloxanes (Sylgaard 184; $\rho = 1.04$ g cm^{-3}) and epoxy resins (Epotek, $\rho = 1.17$ g cm^{-3}).

The prepolymer droplets spread on the substrate until they meet and coalesce into an elongated 'patch'. For droplets to merge, the distance between their centres, d, must be smaller than the sum of

their equilibrium base radii $r_1 + r_2$, where, for a contact angle θ^i_{eq}, $r_i^3 = 3(V/\pi)(1 + \cos\theta_{eq}{}^i) \sin\theta^i_{eq}/[(1 - \cos\theta^i_{eq})(2 + \cos\theta^i_{eq})]$, $i = 1, 2$ and $\cos\theta^i_{eq} = (\sigma_{GS} - \sigma_{SP})/\sigma_{iG}$ (ref. 25). With typical values of contact angles of the prepolymers used, $\theta^i_{eq} \approx 10°$, $r_i \approx 3r_0$.

Both spreading of the droplets and the evolution of the composite patch are driven by surface tension. For typical values of parameters characterizing the droplets (Fig. 2), the Bond number, $Bo = \rho g R h/\sigma_{1,2G}$, describing the balance between the surface tension and the gravitational forces is of the order of 10^{-2} so that the gravity effects can be neglected. When the droplets merge, the composite patch they form evolves to minimize its surface potential energy, $E_{surf} = E_{1G} + E_{2G} + E_{1S} + E_{2S} + E_{12}$, where $E_{1,2G}$ and $E_{1,2S}$ are the surface energies of the polymer–gas and polymer–substrate interfaces, respectively. For similar prepolymers (that is, $\sigma_{1G} \approx \sigma_{2G}$, $\sigma_{1S} \approx \sigma_{2S}$, and $\sigma_{12} \approx 0$), $E_{surf} = (\sigma_{GS} - \sigma_{1S})A_S + \sigma_{1G}A_G$, where A_S and A_G denote, respectively, the total polymer–gelatin and polymer–gas interfacial areas, and σ_{GS} is the surface tension at the solid–gas interface. Because the cohesion forces between the prepolymers and the substrate are strong, the polymer–substrate interface does not recess at any time during the relaxation process (Fig.1a, left column), and the patch is 'pinned' at the ends and expands sideways near its centre. Depending on the volumes and the separation between the droplets, the patch relaxes either into a truncated ellipsoid or a dumbbell shape (Fig. 2b). Quantitatively, an ellipsoidal patch is obtained as long as $\partial E_{surf}(a)/\partial a|_{a=c/2} < 0$, where $2c = 2d$, and $2a$ is the length of the line of contact between the prepolymers. For two prepolymer droplets of identical volumes and of similar wetting characteristics, this condition predicts the critical (maximal) initial distance between the droplets below which they evolve into an ellipsoidal patch: $V/d_{crit}{}^3 \approx \pi[(1 + \cos\theta_{eq})/6]^{1/2}/16$ (see Methods). For the typical droplets we used ($r_0 \approx 250$ μm, $\theta_{eq} \approx 10°$), $d_{crit} \approx 800$ μm, in good agreement with experiment.

The shape of the patch determines whether it will subsequently fold into one composite sphere. Whereas dumbbells always break into smaller droplets during folding, the stability of the ellipsoidal patches is determined by mechanical stability conditions (see above).

The folding process begins when the prepolymer patch is immersed in a liquid isodense with it (usually, an aqueous solution of NaCl or $MnCl_2$; Figs 1a, 2a). This liquid dissolves the gelatin support at a speed of $v = 2$–3 μm s^{-1} and underetches the patch symmetrically from its perimeter inwards. Because the buoyant force acting on the immersed patch compensates the force of gravity, the patch readjusts its shape so as to minimize its interfacial energy—in other words, it folds into a truncated spheroid and, ultimately, into a sphere. At every stage of folding, the patch assumes an equilibrium shape because the capillary time, $\tau_c = \eta d_{char}/2\sigma_{1,2W}$ ($\eta \approx 10$ Pa s, and $d_{char} \approx d \approx 0.5$ mm is the characteristic size of the patch) is of the order of 10^{-2} s and much smaller than the time needed to dissolve the gel under the patch (~1–3 min). This, in turn, implies that gel dissolution does not cause the break-up of the folding patch. As observed experimentally, however, such break-up can occur at the end of the process, when the patch is almost fully detached from the surface, and the polymer–substrate interface is reduced to a line of length L. At this moment, fluctuations of the patch's surface can lead to Rayleigh instabilities and, consequently, the splitting of the patch (Fig. 2a, left column). The folding process is stable against the fluctuations if the distance L is smaller than L_{crit}, given by the condition (see Methods) $V/L^3_{crit} \approx (1/3\pi + 1/2)/4\pi$. As an example, composite spheres of diameters ~500 μm fold from patches for which $L < L_{crit} \approx 880$ μm. In general, the more elongated the patch, the more likely it is to break up on folding.

The method is not limited to self-assembly of droplets from prepolymers of equal densities, and can tolerate density differences up to about 10% (for example, PDMS and epoxy resins; Figs 3,4). Although these differences can be neglected during spreading, they have important consequences for the stability of the patch during folding. First, the density of the salt solution, ρ_L, must be adjusted to the volume-weighted average of the prepolymers merging into a patch, or else the patch detaches from and drifts away from the surface. Second, even for properly adjusted density, folding of the patch is asymmetric (Fig. 2a, right column). Because the buoyancy force on the less dense of the two prepolymers is larger, it lifts from the surface more rapidly, and the patch evolves into a droplet with the lighter prepolymer occupying its top portion. The stability and shape of this structure depend on its size. Small composite droplets are spherical (surface tension dominates buoyancy). As the size grows, hydrostatic forces become important, and the composite droplet takes on a slightly elongated shape and becomes unstable against fluctuations of the prepolymer–liquid interface (so that it can 'neck' and break: Fig. 2a right column and Fig. 2c). For two prepolymers of different densities and equal volumes, and for $\rho_L = (\rho_1 + \rho_2)/2$, stability analysis (see Methods) predicts the maximal (critical) size of the stable composite drop to be $R^2_{crit} \approx 3[4(\sigma_{1,W} + \sigma_{2,W})/3 - 3\sigma_{12}/2]/g(\rho_2 - \rho_1)$. In the case of

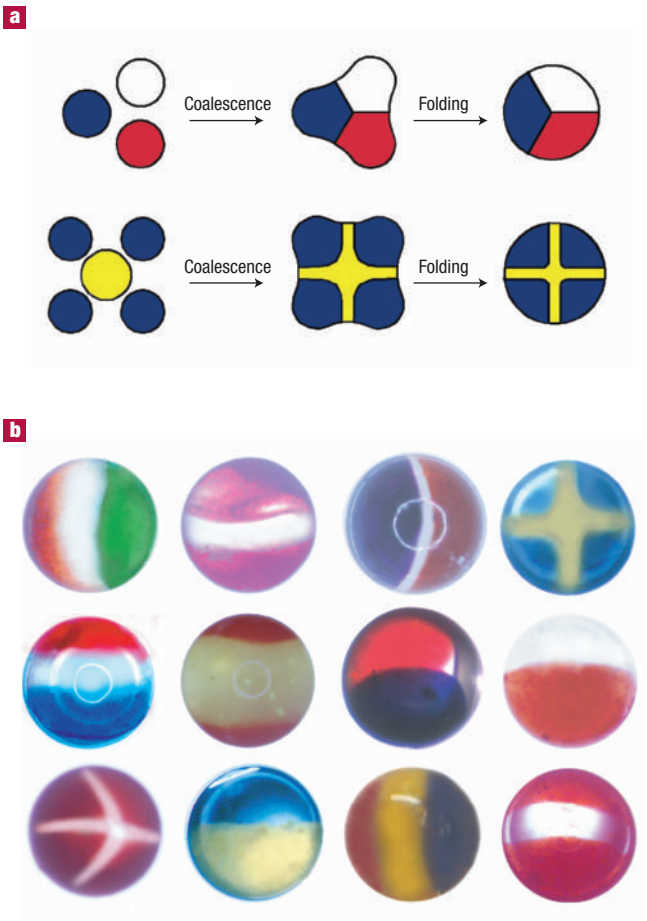

Figure 3 Microspheres with national-flag topologies. **a**, Preparation of Czech flag and Swedish flag microspheres (viewed in the direction perpendicular to the plane of the support). **b**, Collage of optical micrographs of various 'flag' microspheres. From top left to bottom right: Italy, Latvia, France, Sweden, Holland, Spain, Czech Republic, Poland, Switzerland, Ukraine, Belgium and Austria. The smallest (Polish) bead is ~160 μm in diameter; the largest (Swedish) is ~650 μm. Beads are made of various combinations of NOA adhesives and PDMS doped with organic dyes, for example in the Czech bead the clear portion is made of PDMS, the red from NOA81 (Sudan Red) and the blue from NOA63 (Crystal Violet).

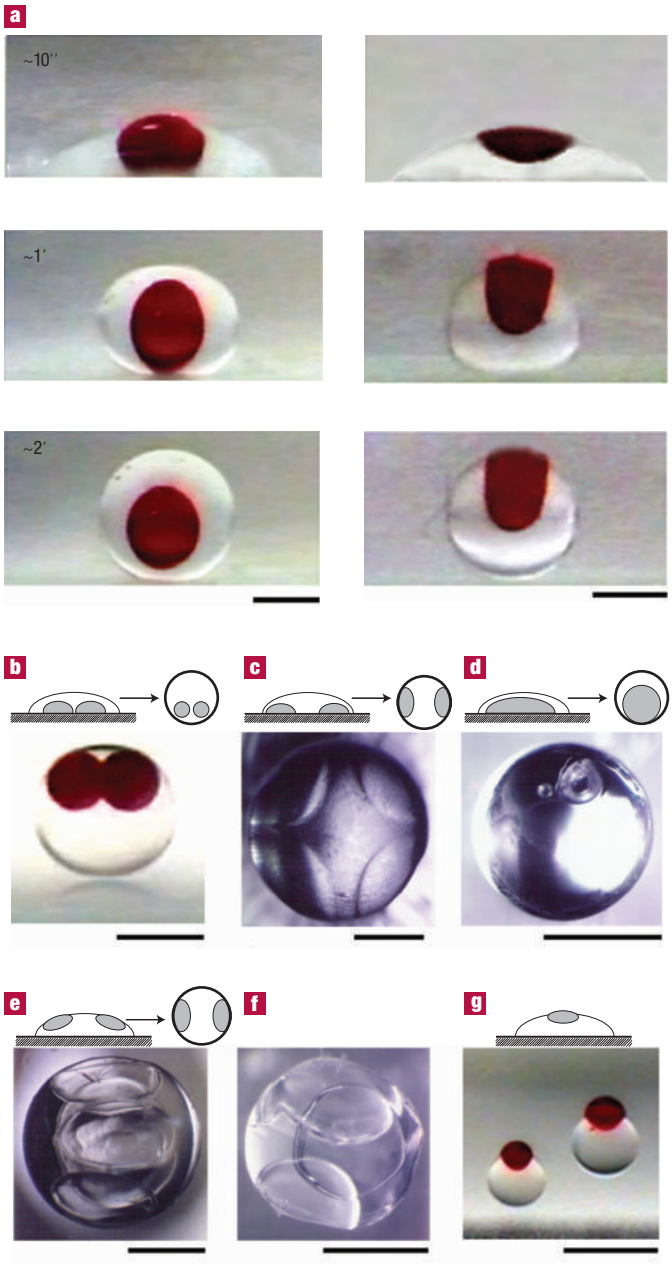

Figure 4 Multicomponent core-and-shell and non-spherical particles. **a**, Folding of epoxy–NOA beads. Left column: clear NOA applied over epoxy dyed with Sudan Red; right column: dyed epoxy applied over clear NOA. The numbers represent time since the initiation of the folding process. **b**, Two-nucleus bead prepared from dyed NOA63 and clear NOA81. **c**, Four-capsule sphere with solidified NOA73 core and thin film covering liquid epoxy patches. **d**, A solid NOA73 shell encasing liquid epoxy. **e**,**f**, Solid PDMS spheres with side-patches of liquid epoxy washed off. The particle in **e** has five patches, and that in **f**, three. **g**, 'Perfume-bottle' particles made of dyed PDMS and clear NOA63. Lighter PDMS 'necks' away from the NOA spheres. The density of the solution is slightly higher than the average density of the particles, so that they detach from the support and slowly drift upwards. All scale bars correspond to 250 μm. Schematic pictures above **b–g** illustrate the arrangements in which the prepolymers were delivered onto the surface or on top of one another. Note the difference between **c** and **e**—in the latter case, the non-curable epoxy was delivered on top of PDMS, and a PDMS film did not cover the liquid epoxy patches in the folded sphere.

two-component PDMS/NOA spheres, the theoretical value of R_{crit} is of the order of a few millimetres; the largest spheres actually made were ~2 mm in diameter.

Patches obtained from the spreading and fusion of several prepolymer droplets fold into multicomponent spheres of D_h symmetries (Fig. 3). The geometries of the folded, composite spheres are uniquely determined by the arrangement and the sizes of the individual droplets printed on the surface. For example, the 'Italian flag' microsphere (top left in Fig. 3b) is prepared by applying three appropriately coloured droplets along a line joining their centres. The 'Czech flag' (Fig. 3a and b) forms from three droplets of equal volumes delivered onto a surface at the vertices of an equilateral triangle. The complex 'Swedish' microbead is prepared by printing four smaller droplets (coloured blue) at the vertices of a square around a larger, yellow droplet; all five droplets merge into an approximately square patch with the yellow one now extended into a cross (Fig. 3a and b).

As in the case of two-component spheres, the formation of a multicomponent patch that does not break up during folding depends on the distances between individual droplets and on the material properties of the prepolymers. Specifically, the distances should be such that for any pair of individual droplets i, j that are supposed to merge, $r_i + r_j > d_{ij}$ and $r_i + r_j \approx d_{crit}$. (the 'necking' condition is less stringent in compact patches). Stability against fluctuations during folding has to be determined numerically; qualitatively, compact patches (for example, the 'Czech flag' patch) are more stable than elongated ones (for example, the 'Italian flag').

Prepolymers can be printed side-by-side or on top of one another. For two-component spheres, there are two distinct possibilities: (i) if a larger droplet is printed onto a smaller one and covers it completely, the composite patch folds into a core-and-shell bead (Fig. 4a, left column); (ii) if a smaller droplet is delivered onto a larger one to give a 'poached egg' patch, it evolves into a globule reaching the top surface of the resultant microsphere (Fig. 4a, right column).

Combination of horizontal and vertical printing permits a virtually unlimited number of topological variations. For example, by applying a large droplet on top of two smaller ones, a two-nucleus bead is obtained (Fig. 4b, top left). If a large patch of a curable prepolymer is printed on top of four smaller droplets of non-curable prepolymers, the folded bead cures into a capsule with a solid core and thin walls containing the non-cured liquids (Fig. 4b, top middle). Conversely, if small droplets of non-curable prepolymers are delivered onto a large droplet of a curable prepolymer, only the core of the folded sphere is solidified; the uncured prepolymer from the side pockets can be washed away to leave behind a carved-out structure (Fig. 4b, bottom left and bottom middle).

Although the maximum dimensions of the spheres are determined by mechanical stability conditions, scaling to smaller sizes (micrometres or even nanometres) is, to the first approximation, determined by the relationship between the capillary time τ_c and the time of etching, $\tau_{etch} = d_{crit}/v$. As long as $\tau_c/\tau_{etch} << 1$, a patch can relax its shape during folding and evolve into a sphere. Because both times scale linearly with d_{char}, we expect the lower size limit to depend only on the material properties of the prepolymers and the speed of etching; mathematically, the condition for proper folding is expressed by $\eta v/2\sigma_{1,2W} << 1$ (~0.003 in our experiments). We also note that smaller droplets should be more stable against possible vibrations than larger ones. To show this, we consider the characteristic time of the droplet's oscillation, τ_{osc}, which scales with the radius R of the droplet as $\tau_{osc} \propto \sqrt{R^3\rho/\sigma}$. At the same time, the characteristic time, τ_{dis}, needed for a vibrating droplet to dissipate its energy, can be estimated from the droplet's energy, $E \sim \rho R^3 v^2$, and the dissipation rate (the Rayleigh function) written as $D \sim \eta R v^2$, with v being the characteristic velocity of the liquid in the droplet. The dissipation time is calculated from the condition $D\tau_{dis} = E$, and

scales with the radius according to $\tau_{dis} \propto R^2\rho/\eta$; for a micrometre-sized droplet, $\tau_{osc} \approx 10^{-4}$ s and $\tau_{dis} \approx 10^{-9}$ s. This means that the characteristic dissipation time is about five orders of magnitude smaller than the characteristic time of possible droplet vibration. In other words, a small drop of viscous prepolymer liquid cannot vibrate because it damps the vibrations instantaneously. In addition, because $\tau_{dis}/\tau_{osc} \sim R^{1/2}$ it also follows that the smaller a droplet the more stable against vibrations it is, and the better it folds.

Of course, printing very small droplets would require a delivery system more elaborate than that we used. An inkjet printer capable of delivering viscous drops would be ideal; although not yet widely available, such printers have already been developed and used in industry. It should be noted, however, that inkjet printing of micrometre-sized patches might not be efficient in producing large, technologically relevant quantities of the microspheres. In this context, the applicability of our method would depend crucially on the speed of serial delivery of the prepolymers. The technique we described can be further extended to making spheroidal and pear-shaped particles by adjusting the density of the salt solutions and of the prepolymers (Fig. 4b, bottom right). Provided that the sizes of the complex particles could be scaled down to colloidal dimensions, the spherical and less-symmetric microparticles should be useful in colloidal self-assembly, optics and controlled-delivery applications. The theoretical analysis that we have presented provides a framework for further study of the coalescence and evolution of multicomponent polymer patches in various environments.

METHODS

SHAPE OF SPREADING PATCH

The shape of the patch formed from two droplets of equal volume V and spaced by d (centre-to-centre) is approximated by an ellipsoidal cup of long axis $2c$, short axis $2a$ and height h (Fig. 2b). Assuming that h is small compared with both c and a, the volume ($2V$) of the patch is given by $2V \approx \pi ach/2$, and the areas of the polymer–substrate and polymer–gas interfaces are $A_S \approx \pi ac$, and $A_G \approx \pi ac(1 + 2h^2/a^2)$, respectively. During relaxation, c is constant, and the decrease of the surface energy, E_{surf}, is due to the increase in the length of the short axis, a. For similar prepolymers, $E_{surf}(a) = (\sigma_{GS} - \sigma_{1S})A_S(a) + \sigma_{1G}A_G(a,h(a))$, where $h(a) = 4V/\pi ac$. The patch evolves into an ellipsoidal cup if $\partial E_{surf}(a)/\partial a|_{a=d/2} < 0$. Differentiation of the surface energy functional yields $V/d_{crit}^3 \approx \pi((1 + \cos\theta_{eq})/6)^{1/2}/16$.

STABILITY OF A PATCH DURING FOLDING

Two similar prepolymers. Just before completely folding up from the surface, a two-component patch has a capsule shape and is attached to the surface at the contact line of length L (Fig. 2a, left column; if the patch were initially circular, this line would reduce to a point). This capsule, approximated by a spherocylinder of radius ζ and length L of cylinder between the hemispheres, is stable against Plateau–Rayleigh-type[26,27] surface instabilities as long as the ratio L/ζ is smaller than 2π; for $L/\zeta > 2\pi$ the patch breaks into two smaller droplets. For a given volume, V, of the droplets forming the patch, the critical length, L_{crit}, of the cylinder is found by applying a sinusoidal surface perturbation along the cylinder's axis $\zeta \to \zeta + \varepsilon \sin(2\pi x/L)$; this procedure gives $V/L_{crit}^3 = (1/3\pi + 1/2)/4\pi$.

Two different prepolymers. Two prepolymers of different densities, $\rho_1 > \rho_2$, and equal volumes fold into a sphere of radius R, in which the less dense prepolymer occupies the top hemisphere. Hydrostatic forces induce deformations of the composite sphere, stretch it along the z-direction, and tend to separate its top and bottom portions (Fig. 2a, right column and Fig. 2c). In the spherical coordinate system, in which the surface of the patch is described by angles θ and φ as ($x = R\sin\theta\cos\varphi$, $y = R\sin\theta\sin\varphi$, $z = R + R\cos\theta$), the simplest, axisymmetric perturbation of the surface that preserves the enclosed volume is of the form: $\delta R(\theta) = \varepsilon(\cos2\theta + 3/5)$, where ε is the amplitude of the deformation. The increment of the surface energy, E_{surf}, caused by the deformation is written as $\delta E_{surf} = 4\pi R\varepsilon[4(\sigma_{1,W} + \sigma_{2,W})/3 - 3\sigma_{12}/2]/5$, where $\sigma_{i,W}$ and σ_{12} denote, respectively, the prepolymer–solution surface tensions and the surface tension at the prepolymer–prepolymer interface. Assuming that the density of the solvent is an arithmetic average of ρ_1 and ρ_2, the decrement of the gravitational energy, E_g, is $\delta E_g = 4\pi gR^3\varepsilon(\rho_1 - \rho_2)/15$, where g is the gravitational constant. Stability condition requires that $\delta E_{surf} > \delta E_g$, and yields the value of the critical radius, R_{crit}, of the composite sphere $R_{crit}^2 = 3[4(\sigma_{1,W} + \sigma_{2,W})/3 - 3\sigma_{12}/2]/g(\rho_2 - \rho_1)$. When R is smaller than R_{crit} the sphere is stable against fluctuations of its surface and does not break into two parts during folding.

Received 6 August 2004; accepted 4 October 2004; published 19 December 2004.

References

1. Yu, Z. R. & Bradley, M. Solid supports for combinatorial chemistry. *Curr. Opin. Chem. Biol.* **6,** 347–352 (2002).
2. Jeong, B., Bae, Y. H., Lee, D. S. & Kim, S. W. Biodegradable block copolymers as injectable drug-delivery systems. *Nature* **388,** 860–862 (1997).
3. Park, S. H., Gates, B. & Xia, Y. *Adv. Mater.* **11,** 462–466 (1999).
4. Terray, A., Oakey, J. & Marr, D. W. M. Microfluidic control using colloidal devices. *Science* **296,** 1841–1844 (2002).
5. Bangs, L. B. New developments in particle-based immunoassays: Introduction. *Pure Appl. Chem.* **68,** 1873–1879 (1996).
6. Russel, W. B., Saville, D. A. & Schwalter, W. R. *Colloidal Dispersions* (Cambridge Univ. Press, Cambridge, 1989).
7. Hunter, R. J. *Introduction to Modern Colloidal Science* (Oxford Univ. Press, Oxford, 1993)
8. Peng, Q., Dong, Y. J. & Li, Y. D. ZnSe semiconductor hollow microspheres. *Angew. Chem. Int. Edn* **42,** 3027–3030 (2003).
9. Fowler, C. E., Khushalani, D. & Mann, S. Interfacial synthesis of hollow microspheres of mesostructured silica. *Chem. Commun.* **19,** 2028–2029 (2001).
10. Yin, J. L. *et al.* Preparation of polystyrene/zirconia core-shell microspheres and zirconia hollow shells. *Inorg. Chem. Commun.* **6,** 942–945 (2003).
11. Xiao, X. C., Chu, L. Y., Chen. W. M., Wang, S. & Li, Y. Positively thermo-sensitive monodisperse core-shell microspheres. *Adv. Funct. Mater.* **13,** 847–852 (2003).
12. Lu,Y., Yin,Y., Li, Z.-Y. & Xia, Y. Colloidal crystals made of polystyrene spheroids: fabrication and structural/optical characterization *Langmuir* **18,** 7722–7727 (2002).
13. Lean, R. C. Physics and performance optimization of electronic paper. *J. Imaging Sci. Tech.* **46,** 562–574 (2002).
14. Hays, D. A. Paper documents via the electrostatic control of particles. *J. Electrostatics* **51,** 57–63 (2001).
15. Wang, J., Liu, G. & Rivas, G. Encoded beads for electrochemical identification. *Anal. Chem.* **75,** 4667–4671 (2003).
16. Fujimoto, K., Nakahama, K., Shidara, M. & Kawaguchi, H. Preparation of unsymmetrical microspheres at the interfaces. *Langmuir* **15,** 4630–4635 (1999).
17. Hugonnot, E., Carles, A., Delville, M. H., Panizza, P. & Delville, J. P. 'Smart' surface dissymmetrization of microparticles driven by laser photochemical deposition. *Langmuir* **19,** 226–229 (2003).
18. Takei, H. & Shimizu, N. Gradient sensitive microscopic probes prepared by gold evaporation and chemisorption on latex spheres. *Langmuir* **13,** 1865–1868 (1997).
19. Nakahama, K., Kawaguchi, H. & Fujimoto, K. A novel preparation of nonsymmetrical microspheres using the Langmuir–Blodgett technique. *Langmuir* **16,** 7882–7886 (2000).
20. Whitesides, G. M. & Grzybowski, B. A. Self-assembly at all scales. *Science* **295,** 2418–2421 (2002).
21. Kim, E. & Whitesides, G. M. Use of minimal free energy and self-assembly to form shapes. *Chem. Mater.* **7,** 1257–1264 (1995).
22. Aubouy, M., Manghi, M. & Raphaël, E. Interfacial properties of polymeric liquids. *Phys. Rev. Lett.* **84,** 4858–4861 (2000).
23. Dee G. T. & Sauer B. B. The surface tension of polymer blends: theory and experiment. *Macromolecules* **26,** 2771–2778 (1992).
24. Karim, A. *et al.* Phase-separation-induced surface patterns in thin polymer blend films. *Macromolecules* **31,** 857–862 (1998).
25. de Ruijter, M. J. & Beysens, D. Droplet spreading: partial wetting regime revisited. *Langmuir* **15,** 2209–2216 (1998).
26. Rayleigh, J. W. S. On the instability of jets. *Proc. London Math. Soc.* **X,** 4–13 (1879).
27. Barbosa, J. & Manfredo, C. Stability of hypersurfaces with constant mean curvature. *Math. Z.* **185,** 339–353 (1984).

Acknowledgements

B.G. gratefully acknowledges financial support from Northwestern University start-up funds and from the Camille and Henry Dreyfus New Faculty Awards Program. M.F. was supported by the NATO Scientific Fellowship. A.B. acknowledges financial assistance from the ProChimia Poland Research Fund. Correspondence and requests for materials should be addressed to B.G.

Competing financial interests

The authors declare that they have no competing financial interests.